

A Structural, Thermogravimetric, Magnetic, Electron Spin Resonance, and Optical Reflectance Study of the $\text{NbO}_x\text{-TiO}_2$ System

M. VALIGI,* D. CORDISCHI, G. MINELLI, P. NATALE,
AND P. PORTA

Centro di Studio CNR su "Struttura ed Attività Catalitica di Sistemi di Ossidi," Dipartimento di Chimica, Università di Roma, 00185 Rome, Italy

AND C. P. KEIJZERS

Department of Molecular Spectroscopy, University of Nijmegen, Toernooiveld, 6525 ED Nijmegen, The Netherlands

Received February 18, 1988; in revised form June 16, 1988

Titanium dioxide samples containing niobium (up to 10%), heated at 1223 K *in vacuo* and subsequently in air, have been investigated by X-ray diffraction, thermogravimetry, magnetic susceptibility measurements, electron spin resonance, and optical reflectance spectroscopy. The results show that for the samples prepared *in vacuo*, niobium is incorporated as Nb(V) compensated by an equivalent amount of Ti(III). The analysis of the magnetic data reveals that some Ti(III) are paired giving a metal-metal interaction. On subsequent heating in air the Ti(III) ions are oxidized to Ti(IV), with the Nb(V) in solid solution being compensated by cation vacancies. The maximum amount of Nb(V) that may be accommodated in the rutile structure is 6.6 Nb atoms/100 Ti atoms. The niobium in excess reacts with TiO_2 giving TiNb_2O_7 . The effect of the various incorporated species on the TiO_2 unit-cell volume is discussed. © 1988 Academic Press, Inc.

Introduction

Titanium dioxide and its solid solutions are currently of interest in several areas of technological and scientific relevance such as solid state chemistry (1), surface chemistry (2), heterogeneous catalysis (3), and more specifically, for applications in photoassisted processes (4). One of the systems which has received a good deal of attention is niobia-titania. Niobium-doped TiO_2 is currently investigated as a pho-

toanode (5), but a full understanding of its photoelectrochemical behavior requires a detailed characterization of the system. In the past, $\text{NbO}_x\text{-TiO}_2$ samples of various compositions and preparations were studied (6-13). However, some questions are still open, such as the oxidation state of niobium, which may in principle be Nb(IV), $4d^1$, or Nb(V), $4d^0$, the dispersion degree, and the extent of magnetic interactions of the incorporated species. These aspects are strictly related to one another, because by dissolving transition metal ions of suitable electronic configuration in rutile TiO_2 , a

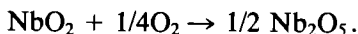
* To whom correspondence should be addressed.

metal-metal interaction occurs (14-16) even at high dilution (17), and affects the dispersion and the magnetic properties.

In the present paper, samples containing niobium (up to 10%) have been examined to confirm the formation of a solid solution, to clarify the role of the atmosphere on the predominant defective situation, and to gain a deeper insight into the oxidation state and on the dispersion degree of the guest ions in the host matrix. The study has been performed by X-ray diffraction, thermogravimetry, electron spin resonance (ESR), optical reflectance spectroscopy, and magnetic susceptibility measurements.

Experimental

Samples. The samples were prepared from niobium and titanium dioxides. Before use, NbO₂ (Ventron) was studied by X-ray diffraction and thermogravimetry: the X-ray powder pattern was found to correspond to that of NbO₂ (18). On thermogravimetry in oxygen the weight was found to increase by 6.48% in the temperature range 523-773 K. This value corresponds to the weight increase (6.40%) expected for the reaction



Titanium dioxide, supplied by Tioxide Int. Ltd. (stated impurities in ppm.: CaO < 20, Zn < 20, Fe < 20, Sn < 20, Al₂O₃ < 100, SiO₂ < 100, K₂O < 10, Nb₂O₅ < 30, Sb₂O₃ < 90, Cl < 50, Na ≈ 180), was heated in air at 673 K, for 2 hr to remove most of the water. The niobium-doped titanium dioxide samples were prepared by mixing weighed amounts of TiO₂ and NbO₂ in an acetone slurry by prolonged grinding in an agate mortar. The acetone was then removed by heating at 473 K in air for 2 hr and the dried powder was pelleted (approximately 500 MPa). The pellets were subjected to two different heat treatments called A and B, respectively. In treatment A the pellets

were sealed inside an evacuated silica tube and gradually heated at 873 K for 24 hr, 1073 K for 24 hr, and 1223 K for 96 hr. The silica tube was then cooled to room temperature and the pellets were exposed to air. In treatment B, some pellets, after treatment A, were again heated in air at 1223 K for 5 hr and then cooled to room temperature. Pellets of pure TiO₂ were treated by the same procedure (A and B) as used for the doped materials. The samples appeared of different color depending on the treatment. Niobium-containing samples, treatment A, are blue with a color intensity increasing with niobium content, while those subjected to treatment B are white. Undoped TiO₂ appears slightly gray and white if subjected to treatments A and B, respectively. The samples containing niobium are designated TNb *X*, the figure *X* after the letters indicates the nominal niobium content derived from the initial composition and expressed as niobium atoms per 100 titanium atoms. The letters A and B denote the thermal treatment.

X-ray. A Debye-Scherrer camera (i.d. = 114.6 mm) was used to obtain the powder diffraction patterns. Unit-cell parameters of TiO₂ were measured with CoK α (Fe-filtered) radiation, as previously described (19). Phase analysis was carried out with CuK α (Ni-filtered) radiation.

Magnetic measurements. The magnetic susceptibility was measured by the Gouy method at 4000, 6000, and 8000 Gauss in a temperature range 78-300 K. A semimicrobalance precise to ± 0.05 mg was employed. The instrument was calibrated with Hg(Co(NCS)₄) (20). The magnetic susceptibility of undoped TiO₂ was determined with the same apparatus. Details of the measurements are reported elsewhere (14).

Thermogravimetric measurements. These were performed in flowing oxygen (25 ml min⁻¹) by a Cahn RG electrobalance. The temperature was raised linearly from room temperature to 1273 K (3° min⁻¹).

TABLE I
X-RAY DIFFRACTION DATA FOR NIOBIUM-DOPED
TiO₂ SAMPLES

Samples ^a	Nb ^b	<i>a</i> (Å)	<i>C</i>	Phases ^c
TiO ₂ A	—	4.5923	0.6443	R
TNb 0.5 A	0.49	4.5936	0.6444	R
TNb 3 A	3.02	4.5972	0.6442	R
TNb 4 A	4.16	4.5999	0.6440	R
TNb 5 A	5.29	4.6040	0.6439	R
TNb 6 A	5.80	4.6027	0.6437	R
TNb 8 A	8.08	4.6108	0.6438	R
TNb 10 A	9.96	4.6182	0.6432	R
TiO ₂ B	—	4.5926	0.6443	R
TNb 1.5 B	1.54	4.5937	0.6442	R
TNb 3 B	3.02	4.5968	0.6441	R
TNb 5 B	5.29	4.6025	0.6435	R
TNb 10 B	9.96	4.6055	0.6430	R, TiNb ₂ O ₇
TNb 11 B	11.16	4.6053	0.6432	R, TiNb ₂ O ₇

^a For designation of samples see text.

^b Concentrations expressed as niobium atoms/100 titanium atoms.

^c R = Rutile.

Diffuse reflectance. Diffuse reflectance spectra were recorded on a Beckman DK 1 instrument in the range 2500–220 nm at room temperature with MgO as reference.

ESR measurements. ESR spectra were obtained at X-band (≈ 9 GHz) using a Varian E-9 spectrometer at 77 K and a Varian E-12 spectrometer at lower temperatures with an Oxford Instrument continuous-flow cryostat BK ESR 12.

Results

X-ray. Only rutile lines were found in the powder X-ray diffraction patterns of TiO₂ A, TiO₂ B, and TNb A (Table I). For the samples of the B series the same situation is observed up to TNb 5 B. In the X-ray diffraction pattern of more concentrated specimens the reflections of TiNb₂O₇ (18) are also present. Table I shows the unit-cell parameter *a* and the axial ratio $C = c/a$. For TiO₂ A and TiO₂ B practically the same values of *a* and *C* are observed. For the doped specimens of both series, an increase of the unit-cell parameter *a* and a decrease of the axial ratio *C* are found with increasing

niobium content. However, at the same niobium content, the increase of *a* is lower for the B samples than for the A ones. Moreover, the specimens TNb 10 B and TNb 11 B show the same values of *a* and *C*. Figure 1 shows the variation of the TiO₂ unit-cell volume, $V = a^3C$ vs the niobium content. Some data reported in the literature (6, 7) are also shown. For the samples of series A a linear expansion of the volume *V* is observed in the whole range of concentration studied, whereas for the three more diluted samples of the series B the volume *V* increases linearly with a lower slope, reaching a constant value for the two more concentrated specimens.

Magnetic measurements. The magnetic susceptibility of all samples was field independent. For undoped TiO₂ A and B the specific susceptibility was found to be very small and positive, changing from $1.3 \cdot 10^{-7}$ to $0.9 \cdot 10^{-7}$ emu/g in the range 100–300 K.

To derive the atomic paramagnetic susceptibility, χ_A , for each temperature the specific susceptibility of TiO₂ was taken in due consideration according to a previously described procedure (14). The Curie-

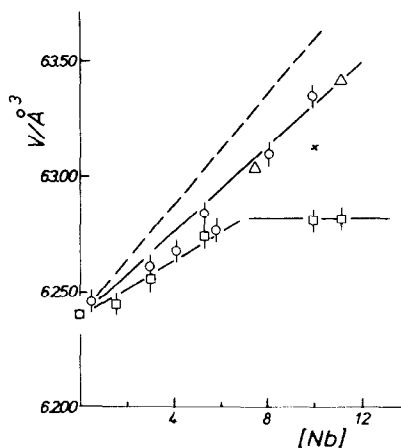


FIG. 1. TiO₂ unit-cell volume, *V*, vs the niobium content, [Nb], expressed as niobium atoms/100 titanium atoms. ---, Calculated line, see text. ○, TNb A; □, TNb B; X, from Ref. (6); △, from Ref. (7).

TABLE II
MAGNETIC DATA FOR THE TNb A SAMPLES

Samples ^a	%Nb ^b	C (emu · K/mole)	- θ (T)	μ_{eff} (BM)
TNb 3 A	3.35	0.447	30	1.89
TNb 4 A	4.54	0.401	35	1.79
TNb 5 A	5.68	0.351	40	1.68
TNb 6 A	6.18	0.366	45	1.71
TNb 10 A	10.01	0.354	65	1.68

^a For designation of samples see text.

^b Concentrations expressed in percentage by weight.

Weiss law was followed for the TNb A samples. For the specimens of the series B, a behavior of the magnetic susceptibility similar to that of undoped TiO₂ was found. Table II collects for the TNb samples the value of the Weiss temperature θ and of the Curie constant C obtained from the intercept on the T -axis and from the slope of χ_A^{-1} against T plots, respectively. The values of the magnetic moment, $\mu_{\text{eff}} = 2.83 C^{1/2}$, are also given. It may be seen that at increasing niobium content a slight increase in the Weiss temperature and a decrease of the μ_{eff} values are observed. This behavior was first reported by Rudorff and Lugisland (7).

Thermogravimetric measurements. No appreciable weight variation was detected on thermograms of undoped TiO₂ A or TiO₂ B as well as on those of the niobium-containing samples of series B. For the TNb A specimens an increase in weight was ob-

served in the temperature range 623 to 1053 K. The weight variation was found to be dependent on the niobium content and is reported in Table III as a percentage, $\Delta\%_{\text{exp.}}^{623-1053}$ together with $\Delta\%_{\text{calc.}}$. The latter quantity is the weight increase calculated by considering the oxidation of Ti(III) to Ti(IV) according to Eq. (4) under discussion.

Diffuse reflectance spectra. Figure 2 shows the spectra of the samples of series A. In addition to the absorption at ≈ 350 nm due to the rutile absorption edge (22), a broad absorption band centered at ≈ 1200 nm ($\approx 8300 \text{ cm}^{-1}$) is observed. Its intensity increases with the niobium content. Figure 3 shows the spectrum of the sample TNb 6A subjected to thermal treatments in air at the specified temperatures for 1 hr. No change is observed for temperatures up to ≈ 600 K, while for higher temperatures the broad absorption intensity decreases and disappears after heating at 873 K.

ESR measurements. At 77 K the ESR spectrum of the more diluted samples (<0.5%) of series A, as well as that of undoped TiO₂ A, show a single asymmetrical line at $g_{\text{av}} = 1.96$ and with a ΔH_{pp} in the

TABLE III
THERMOGRAVIMETRIC DATA FOR THE
TNb A SAMPLES

Samples ^a	%Nb ^b	$\Delta\%_{\text{calc.}}$	$\Delta\%_{\text{exp.}}^{623-1053}$
TNb 4 A	4.54	0.39	0.38
TNb 5 A	5.68	0.49	0.50
TNb 6 A	6.18	0.53	0.52
TNb 10 A	10.01	0.86	0.80

^a For designation of samples see text.

^b Concentrations expressed in percentage by weight.

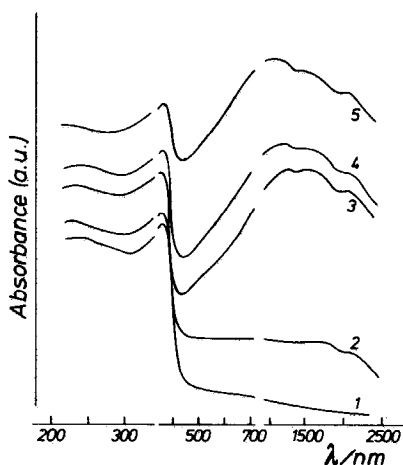


FIG. 2. Reflectance spectra for the TNb A samples. 1, TiO₂ A; 2, TNb 0.5 A; 3, TNb 3 A; 4, TNb 6 A; 5, TNb 10 A.

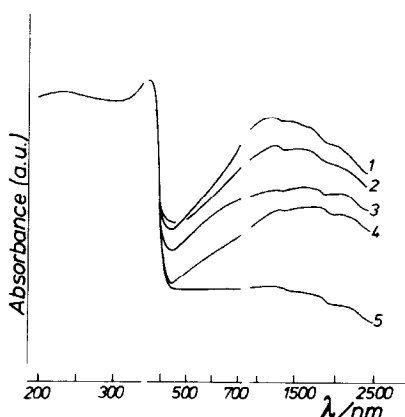


FIG. 3. Reflectance spectra for the sample TNb 6 A heated in air, 1 hr. 1, Untreated; 2, 573 K; 3, 673 K; 4, 773 K; 5, 873 K.

range 60–90 Gauss, the intensity of which increases with the niobium content (Table IV). This signal is strongly dispersive (phase inverted). Moreover, for the more dilute samples a difficulty in tuning the microwave bridge of the ESR spectrometer was found; tuning was no longer possible for samples having a niobium content higher than 0.5%. This behavior is characteristic of conducting materials and indicates that the concentration of mobile defects in the matrix increases with the niobium content. A series of spectra of the sample TNb 0.5 A was recorded at lower temperatures from 4.2 to 67 K. These spectra are reported in Fig. 4. At 4.2 and 39 K a

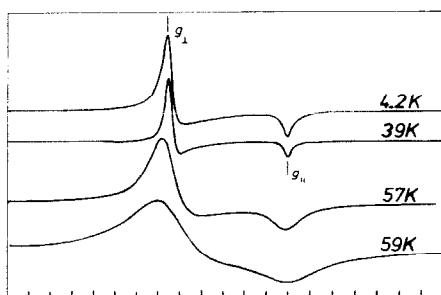


FIG. 4. ESR spectra for the sample TNb 0.5 A recorded at several temperatures. $g_{\perp} = 1.977$; $g_{\parallel} = 1.944$.

very sharp axial signal with $g_{\perp} = 1.977$ and $g_{\parallel} = 1.944$ is observed. By increasing the temperature to 57 and 59 K the spectrum becomes progressively broader and, as reported above, at 77 K it shows a single asymmetrical line. This signal is absent in samples of series B.

Discussion

Samples Heated in Vacuo (TNb A)

The data show that niobium enters in solid solution in the rutile structure. This conclusion, which confirms previous results (6, 7), is inferred from the variation of the TiO₂ unit-cell parameter a and of the axial ratio C (Table I) and from the phase analysis showing that no extra lines other than those of rutile are present in the X-ray diffraction pattern (Table I). In particular, no evidence was obtained for the phase (Nb _{y} Ti _{$(1-y)$})₁₂O₂₉, quoted by Marucco *et al.* (12) for samples treated at 1473 K, $p_{O_2} = 10^{-7}$. We then conclude that within the limit of detectability our samples are single phase.

The question then arises about the oxidation state of the incorporated niobium. To solve this problem, the ESR data will be considered first. The signal at $g = 1.96$ was observed by us (23) several times both on pure and doped (Mn, Rh, Mo, Ru) TiO₂ prepared or treated under reducing conditions (vacuum or hydrogen). This signal has also been reported by others (24–28) and assigned to Ti(III) ions. On the other hand, in single-crystal studies of niobium-doped TiO₂ (rutile) Chester (29) and Zimmermann (30) observed the ESR spectrum of Nb(IV) ion, characterized by a well-resolved hyperfine structure at 4.2 K. In particular, Zimmermann (30) found that the feature of the Nb(IV) spectrum remained unchanged to 17 K; by further increasing the temperature the hyperfine structure gradually coalesced until only a single line was observed

at 25 K. At 50 K the spectrum disappeared. Since the g values of Nb(IV) species in TiO₂ ($g_x = 1.973$; $g_y = 1.981$; $g_z = 1.948$) (30) are very near to those observed on the spectrum of our samples at 4.2 K, it is necessary to discriminate if the spectrum observed for our sample (TNb A 0.5) at 4.2 K is due to Ti(III) or to Nb(IV) species. Computer simulations of powder spectra were performed making use of g and A values of Nb(IV) and of different linewidths. They demonstrated that a hyperfine structure with various degrees of resolution was always present in the calculated spectra, contrary to what is observed experimentally (Fig. 4). Therefore, we assign the signal to Ti(III) ions. This assignment is confirmed also by the different temperature dependence between our spectra and those of Nb(IV) species (30). Further arguments to discriminate between Nb(IV) and Ti(III) come from the magnetic susceptibility data. Following the procedure reported for the parallel case of Ta(IV) and Ti(III) (31), the magnetic susceptibility of Nb(IV) in a distorted octahedral Ti site, as it occurs in TiO₂, may be calculated by the Van Vleck formula (32)

$$\chi_A = (\text{Nb}\beta^2/3KT) [(8 + (3x - 8) \exp(-3x/2)]/[x(2 + \exp(-3x/2))], \quad (1)$$

where $x = \lambda/KT$ and the spin-orbit coupling constant is 750 cm^{-1} (33). This formula is derived in the approximation that $\lambda > V_{\text{or}}$, V_{or} being the potential operator characterizing the orthorhombic distortion of the rutile cationic site. The V_{or} values are estimated to be $300\text{--}400 \text{ cm}^{-1}$ (31). In the case of Ti(III) in the same site, the formula

$$\chi_A = [\text{Ng}^2\beta^2S(S + 1)]/[3K(T - \theta)] \quad (2)$$

must be used since, due to the quite lower spin-orbit coupling constant (for Ti(III) $\lambda = 155 \text{ cm}^{-1}$, i.e., $\lambda < V_{\text{or}}$) the orbital degeneracy of the ground state, ${}^2T_{2g}$, is removed mainly by the site distortion. At 300 and at 100 K, the end values of the temperature

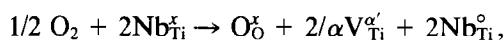
range of our measurements, the following values for χ_A (in emu/mole) are obtained, respectively. For Nb(IV), Eq. (1), $\chi_A = 463 \cdot 10^{-6}$, $\chi_A = 464 \cdot 10^{-6}$. For Ti(III), Eq. (2), taking $g \approx 2$ and $\theta = 0$, $\chi_A = 1250 \cdot 10^{-6}$; $\chi_A = 3751 \cdot 10^{-6}$. Therefore, while for Nb(IV) a practically constant atomic susceptibility is expected, for Ti(III) χ_A increases as the temperature decreases in agreement with the experimental behavior. Moreover, the experimental χ_A values agree with the calculated ones. For example, for TNb 3 (our more dilute sample studied by magnetic susceptibility measurements), the following values were measured: at 300 K, $\chi_A = 1354 \cdot 10^{-6} \text{ emu/mole}$; at 100 K, $\chi_A = 3438 \cdot 10^{-6} \text{ emu/mole}$.

The absence of Nb(IV) and the presence of Ti(III) is also inferred from the reflectance spectra. In fact, when Nb(IV) ($4d^1$ configuration) is incorporated in the Ti(IV) site of the rutile structure, it has a slightly distorted octahedral environment. For pure octahedral symmetry, Nb(IV) is reported to give an absorption band at $\approx 20,000 \text{ cm}^{-1}$ ($\approx 500 \text{ nm}$) (34). No such band was observed in the reflectance spectra of our samples. By contrast, the experimental spectra, Fig. 2, show an intense, very broad absorption with a maximum at lower energy centered at about 8300 cm^{-1} ($\approx 1200 \text{ nm}$). This band is very similar in shape and energy to that appearing in the spectrum of reduced TiO₂ (35). According to Robin and Day (36), such a band is a mixed-valence band of the kind Ti(III)–Ti(IV). Figure 2 shows that the intensity of the broadband increases with the niobium content. Its formation may be accounted for by the following reaction (Kröger symbolism (37)):

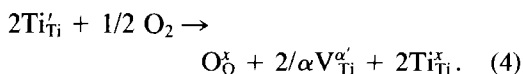


indicating that, in rutile, the substitutionally incorporated Nb(IV), $\text{Nb}_{\text{Ti}}^{\text{IV}}$, reacting with Ti(III) in a lattice site, $\text{Ti}_{\text{Ti}}^{\text{III}}$, gives substitutional Nb(V), $\text{Nb}_{\text{Ti}}^{\text{V}}$, compensated by Ti(III) in a lattice cation site, $\text{Ti}_{\text{Ti}}^{\text{III}}$.

The conclusion we draw from these results, in agreement with literature data (38, 39), is that niobium incorporated in TiO₂ is a donor. The position of the corresponding level is estimated to be only 0.2 eV below the conduction band of TiO₂ (39) and an electron transfer between niobium and titanium may take place according to reaction (3). It must be recalled that under preparation conditions (1273 K and $p_{O_2} = 10^{-7}$ atm) very close to those adopted by us, solid solutions of niobium in titanium dioxide are reported to be metal-deficient systems where cation vacancies are present (12). Therefore together with reaction (3) the following one should also be considered.



where $V_{Ti}^{\alpha'}$ represents a titanium vacancy with α negative charge. However, under our conditions, reaction (3) is by far the predominant one, since, as shown in Table III, the weight increase recorded by heating the sample in an oxygen atmosphere may be accounted for simply by considering the oxidation of the Ti_{Ti}^x formed (reaction (3)) according to the scheme:



The formation of Ti(III) by the incorporation of an equivalent amount of Nb(V) is also in agreement with the ESR and magnetic data. In fact, in the more dilute specimens the signal at $g = 1.96$ assigned to Ti(III) increases in intensity with the niobium content (Table IV). Moreover for low Nb(V) content a low concentration of Ti(III) is present and the magnetic moment is close to the value expected for Ti(III) (40). As the niobium content increases, more Ti(III) ions are produced and Ti(III)-Ti(III) interactions may be possible, thus lowering the value of the magnetic moment (Table II). The decrease of the magnetic

TABLE IV
RELATIVE INTENSITY OF THE SIGNAL AT $g = 1.96$

Samples ^a	ΔH_{pp} ^b (Gauss)	Relative intensity ^b
TiO ₂ A	90	1
TNb 0.05 A	70	1.3
TNb 0.1 A	61	3
TNb 0.2 A	80	5
TNb 0.5 A	60	15

^a For designation of samples see text.

^b Recorded at 77 K (*X*-band).

moment with increasing niobium content was observed also by Rudorff and Lugiand (7) and explained in terms of metal-metal interactions between Nb(IV) ions. Since their samples were prepared under conditions very similar to those adopted in the present paper, we are inclined to think that also in their case Ti(III)-Ti(III) interactions were present. The metal-metal interaction is not unique to solid solutions based on TiO₂, having been observed for other systems, such as, for instance, those based on α -Al₂O₃ (41). However, in the case of rutile (14, 15, 17), it is particularly evident because of the crystal structure of this oxide.

Figure 1 shows the variation of the TiO₂ unit-cell volume with the niobium content. The expansion of V , calculated from the elastic matrix model (42) for the concomitant incorporation of Ti(III) and Nb(V), is also reported (dotted line). The calculation, performed by using the Shannon values for the octahedral ionic radii (43) ($r_{Ti(III)} = 0.67$ Å, $r_{Nb(V)} = 0.64$ Å, $r_{Ti(IV)} = 0.605$ Å), gives higher values than the experimental ones. The discrepancy may be understood by considering that the value for the Nb(V) ionic radius used for the calculation may be inaccurate. Indeed, as reported by Shannon (43), the average Nb(V)-O distance, d , from which the ionic radius is derived, depends on the distortion Δ of the oxygen octahedron according to the relation $d =$

$1.976 + 6.45 \Delta$. The Shannon value implies an average degree of distortion. By assuming that in the solid solutions the oxygen octahedron is distorted as in pure TiO_2 , a value of $\Delta = 0.00011$ is obtained (see Appendix). From this value the average distance $d = 1.977 \text{ \AA}$ is derived and, by subtracting the ionic radius reported for the three-coordinated O^{2-} (1.36 \AA), a value of 0.617 \AA is deduced for the ionic radius of Nb(V). By introducing this corrected value of $r_{\text{Nb(V)}}$ in the calculation of the cell volume variation, a value of 0.092 \AA^3 (for every 1% of niobium) is found, in good agreement with the experimental one ($\Delta V_{1\%}^{\text{exp}} = 0.09 \text{ \AA}^3$).

Samples Heated in Vacuo and Reheated in Oxygen (TNb B)

As shown by the thermogravimetric experiments, when the samples TNb A are heated in oxygen starting from 623 K, Ti(III) oxidizes to Ti(IV). In a parallel fashion, the broad absorption band progressively decreases (Fig. 3), the solid becomes white, and the ESR signal disappears. The oxidation occurs in solid solution and causes a shrinkage of the TiO_2 unit-cell volume (Fig. 1). For samples with niobium content higher than that in TNb 6 the oxidation takes place with segregation of niobium from the solid solution, as shown by the presence of TiNb_2O_7 as a separate phase (Table I) and by the constancy of the TiO_2 unit-cell volume (Fig. 1). From Fig. 1 a solubility limit of 6.6 niobium atoms/100 titanium atoms is inferred. This value compares well with that reported by Eror (10) (6.4 Nb atoms/100 Ti atoms at 1333 K in O_2). Therefore, by applying the elastic matrix model, the expression $\Delta V_{1\%} = K(r_{\text{Nb(V)}}^3 - r_{\text{Ti(IV)}}^3) + x$ may be written, where x stands for the contribution of the compensating cationic defect neutralizing the Nb(V) positive excess charge. By using for Nb(V) the corrected radius (0.617 \AA) a value of $\Delta V_{1\%} = (0.013 + x) \text{ \AA}^3$ is calculated. This value is somewhat lower than

the experimental one, $\Delta V_{1\%}^{\text{exp}} = 0.060 \text{ \AA}^3$ (from Fig. 1, samples with a niobium content lower than the solubility limit). The difference indicates a contribution of the compensating defect. In ionic solids, lattice vacancies are known to cause a lattice expansion (44, 45). Although TiO_2 is believed not to be a purely ionic solid, it is reasonable to expect a positive value for x (expansion) even in the present case.

Conclusion

The data obtained from different techniques show that, depending on the gaseous atmosphere, the incorporation of niobium in TiO_2 causes a different defective situation. For the TNb A samples (heated *in vacuo*) niobium is incorporated as Nb(V) and an equivalent amount of Ti(IV) is transformed to Ti(III). The analysis of the magnetic data reveals that some Ti(III) are paired giving a metal-metal interaction. These results are very similar to those found for the $\text{TaO}_x\text{-TiO}_2$ system where Ta(V) and Ti(III) are reported to be concomitantly present in the TiO_2 structure (46) and where an interaction takes place between Ti(III) and Ti(III) pairs (31). By heating the samples in air (TNb B specimens) the Ti(III) ions are oxidized to Ti(IV) and the incorporated Nb(V) is compensated by cation vacancies. The maximum amount of Nb(V) that may be accommodated in the rutile structure is 6.6 Nb atoms/100 Ti atoms in good agreement with previous studies (10). Niobium in excess with respect to this value reacts with TiO_2 giving TiNb_2O_7 .

Appendix

The oxygen octahedron around a Ti(IV) ion in the rutile structure is slightly distorted. The four equatorial Ti-O distances are $d_1 = 1.944 \text{ \AA}$ while the two apical ones are $d_2 = 1.988 \text{ \AA}$. Therefore the average Ti-O distance, d , is $d = (1/6) \cdot (4 \cdot 1.944 + 2 \cdot 1.988) = 1.959 \text{ \AA}$. For undoped TiO_2 the

distortion degree defined as $\Delta = (1/6)\Sigma((d_i - d)/d)^2$, is 0.00011.

References

1. J. S. ANDERSON, "Surface and Defect Properties of Solids," p. 1, Specialist periodical report, Chem. Soc., London (1972).
2. T. J. WISEMAN, in "Characterization of Powder Surface" (G. D. Parfitt and K. S. W. Sing, Eds.), p. 153, Academic Press, New York/London (1976); E. HERTMAN, *ibid.*, p. 209.
3. G. C. BOND AND R. BURCH, in "Catalysis 6" (G. C. Bond and G. Webb, Eds.), p. 27, Royal Soc. Chem., London (1983).
4. R. I. BICKLEY, in "Catalysis 5" (G. C. Bond and G. Webb, Eds.), p. 308, Royal Soc. Chem., London (1982).
5. Y. MATSUMOTO, T. SHIMIZU, A. TOYODA, AND E. SATO, *J. Phys. Chem.* **86**, 3581 (1982).
6. B. O. MERINDER, E. DORM, AND M. SELEBORG, *Acta Chem. Scand.* **16**, 29 (1962).
7. W. RUDORFF AND H. H. LUGISLAND, *Z. Anorg. Allg. Chem.* **334**, 125 (1964).
8. J. F. BAUMARD AND E. TANI, *J. Chem. Phys.* **67**, 857 (1977).
9. R. T. DIRSTINE AND C. J. ROSA, *Z. Metallkd.* **70**, 372 (1972).
10. N. G. EROR, *J. Solid State Chem.* **38**, 281 (1981).
11. S. K. E. FORGHANY AND J. S. ANDERSON, *J. Solid State Chem.* **40**, 136 (1981).
12. J.-F. MARUCCO, B. POUHELLEC, J. GAUTRON, AND P. LEMASSON, *J. Phys. Chem. Solids* **46**, 709 (1985).
13. B. POUHELLEC, F. LAGUEL, J.-F. MARUCCO, AND B. TOUZELIN, *Phys. Status Solidi B* **133**, 371 (1986).
14. M. VALIGI, D. GAZZOLI, M. LO JACONO, G. MINELLI, AND P. PORTA, *Z. Phys. Chem. N.F.* **132**, 29 (1982).
15. M. VALIGI, S. DE ROSSI, D. GAZZOLI, AND G. MINELLI, *J. Mater. Sci.* **20**, 71 (1985).
16. M. VALIGI, D. GAZZOLI, P. NATALE, AND P. PORTA, *Gazz. Chim. Ital.* **116**, 391 (1986).
17. D. CORDISCHI, D. GAZZOLI, AND M. VALIGI, *Gazz. Chim. Ital.* **113**, 597 (1983).
18. X-ray Powder Data File, ASTM 19-859.
19. M. VALIGI AND A. CIMINO, *J. Solid State Chem.* **12**, 135 (1975).
20. B. N. FIGGIS AND R. S. NYHOLM, *J. Chem. Soc.*, 4190 (1958).
21. X-ray Powder Data File, ASTM 9-258.
22. A. L. COMPANION AND R. F. WYATT, *J. Phys. Chem. Solids* **24**, 1025 (1963).
23. Unpublished results from this laboratory.
24. B. H. CHENA AND J. M. WHITE, *J. Phys. Chem.* **87**, 1327 (1983).
25. B. T. HUIZINGA AND R. PRINS, *J. Phys. Chem.* **85**, 1327 (1981).
26. E. SERWICKA, M. W. SCHLIERKAMP, AND R. N. SCHINDLER, *Z. Naturforsch. A* **36**, 226 (1981).
27. S. A. FAIRHURST, A. D. INGLIS, Y. LE PAGE, J. R. MORTON, AND K. F. PRESTON, *Chem. Phys. Lett.* **95**, 444 (1983).
28. S. A. FAIRHURST, A. D. INGLIS, Y. LE PAGE, J. R. MORTON, AND K. F. PRESTON, *J. Magn. Reson.* **54**, 300 (1983).
29. P. F. CHESTER, *J. Appl. Phys.* **32**, 866 (1961).
30. P. H. ZIMMERMANN, *Phys. Rev. B* **8**, 3917 (1973).
31. A. CASALOT, O. MONNEREAU, AND M. DRILLON, *Mater. Res. Bull.* **12**, 861 (1977).
32. F. E. MABBS AND D. J. MACHIN, "Magnetism and Transition Metal Complexes," Chapman & Hall, London (1973).
33. A. ABRAGAM AND B. BLEANEY, "Electron Paramagnetic Resonance of Transition Metal Ions," p. 474, Oxford Univ. Press (Clarendon), New York/London (1970).
34. A. P. B. LEVER, "Inorganic Electronic Spectroscopy," 2nd ed., p. 392, Studies in Physical and Theoretical Chemistry, No. 33, Elsevier, Amsterdam (1984).
35. V. R. PORTE, W. B. WHITE, AND R. ROY, *J. Solid State Chem.* **4**, 250 (1972).
36. M. B. ROBIN AND P. DAY, Mixed valence chemistry, in "Advances in Inorganic Chemistry and Radiochemistry" Vol. 10, p. 247, Academic Press, New York, (1967).
37. F. A. KRÖGER, "The Chemistry of Imperfect Crystals," North-Holland, Amsterdam (1964).
38. B. POUHELLEC, J.-F. MARUCCO, AND F. LAGNEL, *J. Phys. Chem. Solids* **47**, 381 (1986).
39. B. POUHELLEC, J.-F. MARUCCO, B. CALES, AND B. TOUZULIN, *J. Phys. C* **47**, 825 (1986).
40. B. N. FIGGIS, "Introduction to Ligand Fields," p. 287, Interscience, New York (1967).
41. A. CALLAGHAN, M. J. ROSSITER, AND F. S. STONE, *J. Chem. Soc. Faraday Trans.* 3463 (1966).
42. M. VALIGI AND D. GAZZOLI, *Z. Phys. Chem. N.F.* **125**, 89 (1981).
43. R. D. SHANNON, *Acta Crystallogr. Sect. A* **32**, 751 (1976).
44. N. F. MOTT AND M. J. LITTLETON, *J. Chem. Soc. Faraday Trans.* **34**, 485 (1938).
45. A. CIMINO AND M. MAREZIO, *J. Phys. Chem. Solids* **17**, 57 (1960).
46. O. MONNEREAU AND A. CASALOT, *J. Solid State Chem.* **23**, 399 (1978).